

# The Kinetics of CO Oxidation on RuO<sub>2</sub>(110): Bridging the Pressure Gap

J. Wang, C. Y. Fan, K. Jacobi,\* and G. Ertl

Department of Physical Chemistry, Fritz-Haber-Institut der Max-Planck-Gesellschaft, Faradayweg 4-6, D-14195 Berlin, Germany

Received: November 8, 2001; In Final Form: January 14, 2002

The steady-state rate  $r_{\text{CO}_2}$  of CO<sub>2</sub> formation from CO + O<sub>2</sub> on an epitaxially grown RuO<sub>2</sub>(110) single-crystal surface was recorded as a function of the partial pressures in the 10<sup>-7</sup>–10<sup>-6</sup> mbar range. The RuO<sub>2</sub>(110) surface exposes singly coordinatively unsaturated “Ru-cus” sites and 2-fold coordinatively unsaturated “Ru-bridge” sites. Normally, the Ru-bridge sites are saturated by oxygen (O-bridge) which can be replaced by CO. The stage of the surface was controlled by vibrational spectroscopy (HREELS), and analysis of the kinetic data was based on previous information about the structural and adsorptive properties of this surface. Measurements of the rate as a function of temperature up to ≈350 K in a 1:1 mixture of CO and O<sub>2</sub>, each with 10<sup>-7</sup> mbar partial pressure, revealed most remarkable agreement with data reported by Zang and Kisch<sup>13</sup> with small supported RuO<sub>2</sub> particles prepared from aqueous solution for 1 bar total pressure. Under these conditions of temperature and *ratio* of partial pressures the reaction will essentially proceed between CO and O species adsorbed at Ru-cus. The *total* pressure becomes largely insignificant: whereas the pressure changes by 10 orders of magnitude,  $r_{\text{CO}_2}$  is estimated to vary only within 1 order of magnitude so that the pressure gap is bridged here.

## 1. Introduction

Studies with well-defined single crystal surfaces under UHV conditions enabled to elucidate the microscopic reaction mechanisms underlying heterogeneously catalyzed reactions. The transfer of the results derived along this “surface science” approach to the high-pressure conditions of “real” catalysis could be successfully achieved in a few cases, including, for example, ammonia synthesis on Fe<sup>1</sup> and Ru<sup>2</sup> surfaces, or CO oxidation on Rh.<sup>3</sup> With the latter reaction there existed, however, for long a puzzle: While under UHV conditions Ru is practically inactive,<sup>4</sup> it is even superior to Pt and Pd if the reaction is performed in a gas flow at atmospheric pressure.<sup>5</sup> On the other hand, under the latter conditions the kinetics was shown to be identical for supported small particle catalysts as well as for single crystals,<sup>6</sup> indicating an apparent manifestation of the so-called “pressure gap”.

Recently it could be shown that this effect has in fact to be attributed to a “material gap” as a chemical transformation takes place with a Ru surface under high O<sub>2</sub> exposures: On Ru(0001) a thin epitaxial overlayer of RuO<sub>2</sub> exposing its (110) face is formed. Once this phase has been created it is also stable under UHV conditions and exhibits a high catalytic activity for CO oxidation even down to room temperature due to its specific properties in adsorbing both oxygen and carbon monoxide.<sup>7</sup> The latter were explored in detail in previous studies.<sup>8–12</sup> The present paper now reports on the steady-state kinetics of this reaction with a RuO<sub>2</sub>(110) surface under UHV conditions, where analysis of the data will be based on knowledge about the adsorptive properties of this surface.

On the other hand, there was a recent report on CO oxidation under atmospheric pressure conditions at RuO<sub>2</sub> particles pre-

pared from aqueous solution.<sup>13</sup> It will be shown that comparison of the temperature dependence of the rate for an identical  $p_{\text{CO}}/p_{\text{O}_2}$ -ratio exhibits quite remarkable agreement between both sets of data, despite the fact that the absolute pressure differed by about 10 orders of magnitude! We believe that this represents a clear example for bridging the “pressure gap” so that for this system both a “material” and a “pressure gap” are closed.

## 2. Experimental Section

The experiments were performed in an ultrahigh vacuum (UHV) apparatus consisting of two chambers connected through a valve to allow sample preparation separately. The first chamber with a base pressure of  $4 \times 10^{-11}$  mbar contained facilities for low-energy electron diffraction (LEED), thermal desorption spectroscopy (TDS), and reaction rate measurements by means of a quadrupole mass spectrometer, gas dosing, and sputtering. The second chamber with a base pressure of  $2 \times 10^{-11}$  mbar housed a high-resolution electron energy loss (HREEL) spectrometer. Spectra were taken at an angle of incidence of 60° relative to the surface normal in specular geometry. The primary energy was 3 eV and the resolution was 2.7–3.6 meV.

The RuO<sub>2</sub>(110) surface was prepared epitaxially on a Ru(0001) surface mounted through W wires in narrow slits at the edges of the sample and heated by electron bombardment from the backside. It should be noted, however, that during reaction the heating was performed only by heat radiation from the tungsten filament so that no chemical processes were induced by interaction of electrons with the reacting gases. The RuO<sub>2</sub>(110) surface was produced by exposing  $1 \times 10^7$  L of O<sub>2</sub> at a sample temperature of 700 K. A glass capillary array doser was used at a distance of about 15 mm from the sample, yielding an enhancement of the pressure at the sample surface by a factor of about 30. This procedure resulted in a surface, which was covered by a thin single-crystalline layer of RuO<sub>2</sub>(110) ordered

\* Corresponding author. Fax: +49-30-8413-5106. E-mail address: jacobi@fhi-berlin.mpg.de. WWW: <http://w3.rz-berlin.mpg.de/pc/ElecSpec>.

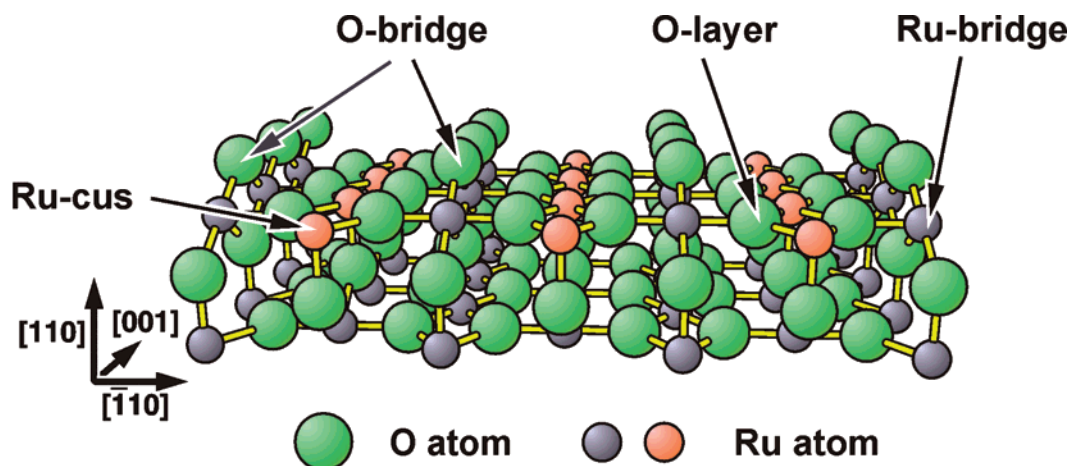


Figure 1. Ball-and-stick model of the RuO<sub>2</sub>(110) surface with empty Ru-cus sites.<sup>7</sup>

in patches of three different domains, rotated laterally by 120° as checked by LEED in accordance with refs 7 and 8. The preparation could be repeated after sputter cleaning the Ru-(0001) substrate.

Steady-state rate measurements were carried out in the first chamber which was operated as a continuous-flow reactor. Reactants (CO and O<sub>2</sub>) were introduced through separate leak valves and were pumped off (together with the product CO<sub>2</sub>) with a turbo-molecular pump. The partial pressures recorded by the mass spectrometer were calibrated against an ionization gauge. Reaction rates (rates of CO<sub>2</sub> formation) were evaluated from the product partial pressure through the equation

$$r_{\text{CO}_2} = \frac{pN_0V}{\tau_A RT_g} \quad (\text{molecules/s}) \quad (\text{I})$$

where  $p$  is the partial pressure of CO<sub>2</sub>,  $V$  the volume of the reactor,  $N_0 = 6.022 \times 10^{23}$  Avogadro's number,  $\tau_A$  the reactor residence time as evaluated from the pumping speed, and  $T_g$  the gas temperature (300 K).

### 3. Results

To rationalize the results of the kinetic measurements, at first the structure model for the clean RuO<sub>2</sub>(110) surface is shown in Figure 1.<sup>7</sup> It exposes two types of Ru atoms, denoted by Ru-cus and Ru-bridge, which can each be occupied by either O (O-cus and O-bridge) or CO (CO-cus and CO-bridge). The energetic and vibrational properties of these various species have been investigated in detail before.<sup>7–10</sup> In brief:

(i) O-cus desorbs around 400 K and occupies up to 80% of the cus sites at 300 K and thereby hinders the formation of CO-cus, which process is however not completely suppressed. The energy of the Ru–O stretch vibration is 103 meV.<sup>8</sup>

(ii) O-bridge desorbs around 1000 K and hinders formation of CO-bridge. It exhibits a stretch vibration at 69 meV.

(iii) CO-cus desorbs around 300 K, i.e., this species will be pumped off above room temperature in vacuo. The energy of its C–O stretch vibration is 262 meV and of its motion against Ru-cus is 39 meV.<sup>9,10</sup>

(iv) CO-bridge desorbs around 450 K and hinders adsorption of O-bridge, but not so efficiently as in the opposite sense because of the marked difference in adsorption energy. This species exhibits two bands for the C–O stretch vibration at 235 and 245 meV and one mode at 52 meV for the CO against Ru-bridge stretch vibration.<sup>9,10</sup>

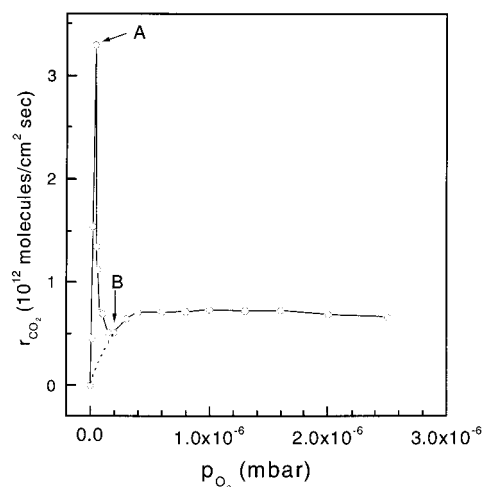
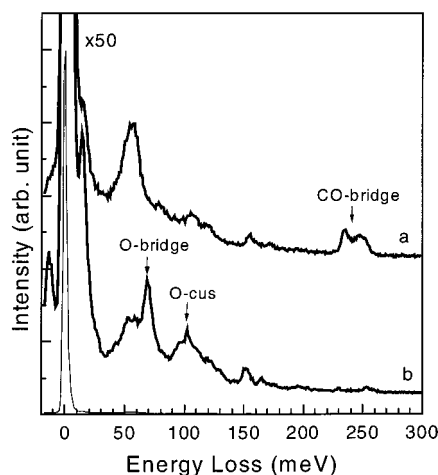


Figure 2. Rate of CO<sub>2</sub> formation,  $r_{\text{CO}_2}$ , on RuO<sub>2</sub>(110) as a function of O<sub>2</sub> partial pressure,  $p_{\text{O}_2}$ , for fixed CO partial pressure,  $p_{\text{CO}} = 1 \times 10^{-7}$  mbar, and  $T = 350$  K.

CO<sub>2</sub> will immediately be released from the surface above room temperature; at 85 K it is characterized by two main vibrational bands at 81 and 291 meV.<sup>14</sup>

The kinetic behavior revealed to be rather complex. Since the rate of CO<sub>2</sub> formation,  $r_{\text{CO}_2}$ , depends on the partial pressures of both CO and O<sub>2</sub> as well as on temperature  $T$ , the data will be presented as function of each one of these parameters while the other two are kept fixed.

**3.1.  $r_{\text{CO}_2}(p_{\text{O}_2})$  at  $p_{\text{CO}} = 1 \times 10^{-7}$  mbar,  $T = 350$  K.**  $T = 350$  K was chosen since this temperature represents under certain aspects an optimum. To suppress background and “memory” effects by too heavy gas loads, the partial pressures of the reactants were usually kept below  $3 \times 10^{-6}$  mbar. The variation of the reaction rate  $r_{\text{CO}_2}$  with the O<sub>2</sub> partial pressure under the stated conditions is reproduced in Figure 2.  $r_{\text{CO}_2}$  at first increases linearly with  $p_{\text{O}_2}$  and reaches a maximum near  $p_{\text{O}_2} = 4 \times 10^{-6}$  mbar, i.e., close to the stoichiometric CO:O<sub>2</sub> composition. The subsequently recorded HREEL spectrum at this point (A) is shown in Figure 3, curve a. The broad peak at about 56 meV is due to a superposition of the CO against Ru-bridge stretch vibration at 52 meV<sup>8</sup> and a multicomponent contribution from the substrate. O-bridge (and O-cus) is completely missing. Since the reaction still takes place during shutting-off the pressure supply, no information about the actual concentration of adsorbed species under reaction conditions is available. However, one can conclude that there is a slight surplus of CO under the chosen conditions so that not all CO-bridge becomes reacted



**Figure 3.** High-resolution electron energy loss spectra (HREELS). Curve a: after interrupting the reaction at point A of Figure 2 ( $p_{O_2} = 4 \times 10^{-8}$  mbar). Curve b: after interrupting the reaction at point B of Figure 2 ( $p_{O_2} = 2 \times 10^{-7}$  mbar).

off as indicated by the presence of the respective bands in the spectrum. Thus, spectrum a in Figure 3 suggests that O-bridge and CO-bridge are the main surface species involved in the reaction under these conditions. Since CO-cus is relatively weakly held on the Ru-cus sites, this species will be pumped off before the HREEL spectrum can be recorded and its possible existence cannot be confirmed.

Further increase of  $p_{O_2}$  causes a decrease of  $r_{CO_2}$  until a minimum is reached around  $p_{O_2} = 2 \times 10^{-7}$  mbar (point B). The HREELS data recorded at this stage (curve b of Figure 3) indicates now the presence of O-bridge and a small amount of O-cus, while the concentration of CO-bridge has been largely suppressed. Hence it is suggested that the reaction is now shifted from the bridge sites to the cus sites. The latter become, however, covered by O atoms only to a maximum of about 80%, so that even at oxygen saturation CO adsorption on the remaining cus-sites is still possible. Further increase of the  $O_2$  partial pressure beyond  $p_{O_2} = 2 \times 10^{-7}$  mbar causes a further (small) rise of  $r_{CO_2}$  until saturation is reached around  $p_{O_2} = 4 \times 10^{-7}$  mbar. It is concluded that the reaction is dominated by interaction between O-cus (covering 80% of the cus sites) and CO-cus. Previous titration experiments have shown that reaction between O-bridge and CO-cus becomes appreciable only when the supply by O-cus is almost exhausted.<sup>9,10</sup>

**3.2.  $r_{CO_2}(p_{CO})$  at  $p_{O_2} = 1 \times 10^{-7}$  mbar,  $T = 350$  K.** The variation of the reaction rate with CO partial pressure is plotted in Figure 4. As becomes clearer from the inset,  $r_{CO_2}(p_{CO})$  takes off slowly and then increases steeply, until a maximum is reached around  $p_{CO} = 2.5 \times 10^{-7}$  mbar, i.e., again near the stoichiometric composition. The HREEL spectrum taken at point A ( $p_{O_2} = 3 \times 10^{-8}$  mbar, curve a of Figure 5) shows the presence of both O-bridge and O-cus. Hence the CO molecules adsorbing on the small fraction of empty Ru-cus sites will preferentially react with neighboring O-cus species. With increasing  $p_{CO}$  the rate rises and the O-cus species will be increasingly consumed. At point B near the maximum the HREEL spectrum shows the presence of a small amount of CO-bridge, while the concentrations of O-bridge and O-cus are suppressed. The reaction is now suggested to essentially occur between O-bridge and CO-bridge (plus transient CO-cus). Again we conclude that about stoichiometric amounts of O-bridge and CO-bridge are adsorbed during reaction so that after shutting-off both species are reacted off until only a slight surplus of CO remains on the surface. Further increase of  $p_{CO}$  then causes

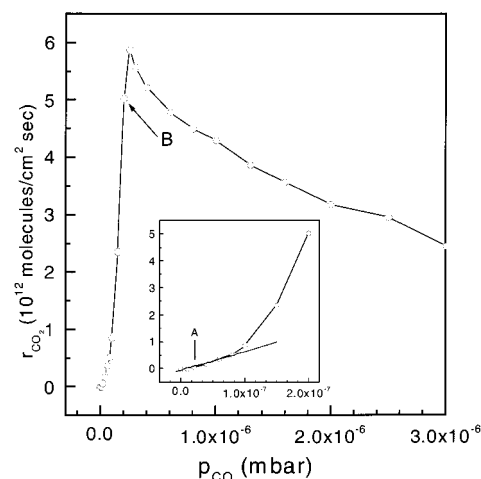


**Figure 4.** Rate of  $CO_2$  formation,  $r_{CO_2}$ , as a function of CO partial pressure,  $p_{CO}$ , for fixed  $p_{O_2} = 1 \times 10^{-7}$  mbar and  $T = 350$  K. The inset shows the initial range on an expanded abscissa scale.

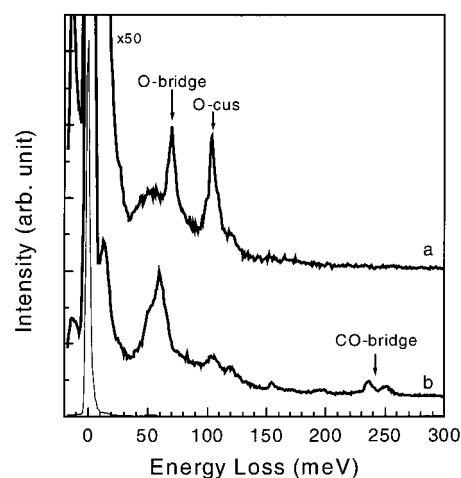


**Figure 5.** HREEL spectra. Curve a: after interrupting the reaction at point A of Figure 4 ( $p_{CO} = 3 \times 10^{-8}$  mbar). Curve b: after interrupting the reaction at point B of Figure 4 ( $p_{CO} = 2 \times 10^{-7}$  mbar).

increasing inhibition of O-bridge formation through site blocking by CO-bridge.

**3.3.  $r_{CO_2}(T)$  for  $p_{CO} = p_{O_2} = 1 \times 10^{-7}$  mbar.** The variation of the reaction rate with temperature for a given gas composition is reproduced in Figure 6 as full dots in the form of an Arrhenius plot. (The open symbols in this figure will be discussed later.) This temperature range is, admittedly, rather narrow for the following reasons: Below room temperature the reaction becomes very sluggish. Above 350 K desorption of CO becomes more noticeable, and this is presumably the reason for the drop in reactivity beyond this temperature. From the linear part of the Arrhenius plot an (apparent) activation energy of about 56 kJ/mol ( $= 0.6$  eV) is derived. The preceding discussion of the results suggests that under these conditions the reaction is essentially taking place between O-cus and CO-cus species.

## 4. Discussion

**4.1. Reaction Mechanism and Kinetics.** Like with transition metal surfaces, the oxidation of CO on  $RuO_2$  proceeds via the Langmuir–Hinshelwood mechanism by interaction between chemisorbed O and CO species, as manifested, for example, by the HREELS data. In contrast, however, both species are present on the surface not only as a single type each, as has been outlined above. Instead (for  $T \leq 350$  K) the following

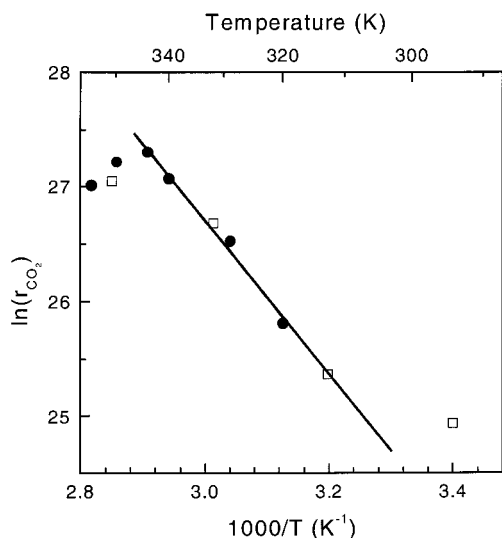
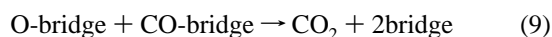
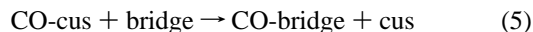
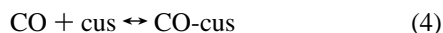
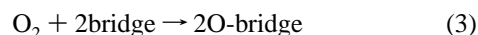
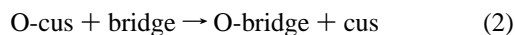


**Figure 6.** Arrhenius plot,  $\ln r_{\text{CO}_2}$  vs  $1/T$ . ●: UHV data for RuO<sub>2</sub>(110) at  $p_{\text{O}_2} = p_{\text{CO}} = 1 \times 10^{-7}$  mbar. □: Data from Zang and Kisch<sup>13</sup> for small RuO<sub>2</sub> particles at  $p_{\text{O}_2} = p_{\text{CO}} = 500$  mbar.

reaction steps have to be formulated (where “cus” refers to the Ru-cus site and “bridge” refers to the Ru-bridge site):



These reactions are further commented as follows:

(1) O<sub>2</sub> may dissociatively adsorb on cus-sites, from where it recombinatively desorbs around 400 K.<sup>8</sup> This process proceeds through dissociation of a molecular precursor which is stable below 140 K and bridges two adjacent Ru-cus atoms.<sup>8</sup> STM images taken at room temperature indicate that the O-cus species appear almost exclusively as pairs (or multiples of pairs) and exhibit rather limited mobility.<sup>15</sup> As a consequence the concentration of sites for dissociative oxygen adsorption will essentially be proportional to the concentration of cus sites. For this reason it is a good approximation to formulate the kinetics of this step as a first-order rate process as done later in eqs 11 and 15.

(2) Since bonding of O to a bridge-site is stronger than on a cus-site, this transition will take place if a neighboring free bridge-site is available.<sup>8</sup>

(3) Direct occupation of bridge-sites through dissociative adsorption of O<sub>2</sub> is unlikely, but cannot be ruled out. It is hard to distinguish from route (1+2). The O-bridge species is rather strongly held and desorbs only around 1000 K.<sup>8</sup>

(4+5) Similarly, CO adsorbs on cus-sites, where it is weakly held and desorbs below 300 K, as well as occupies bridge-sites, from where desorption occurs at about 450 K.<sup>9</sup>

(6–9) In principle, CO<sub>2</sub> formation might take place according to all four routes indicated. At temperatures above 350 K additional complications come into play by the fact that now fully coordinated O-atoms and eventually deeper layers become reacted off.

For these reasons and in view of the results in Figure 6 the following discussion will be restricted to  $T \leq 350$  K and will be more of qualitative nature rather than full kinetic modeling will be attempted.

The complex variation of the rate of CO<sub>2</sub> production,  $r_{\text{CO}_2}$ , with  $p_{\text{O}_2}$  at fixed  $p_{\text{CO}} = 1 \times 10^{-7}$  mbar and  $T = 350$  K, as depicted in Figure 2 can be rationalized as follows, whereby the HREELS data characterizing the state of the surface at points A and B is taken into account: At low  $p_{\text{O}_2}$  the surface will be largely covered by CO-bridge species while the concentration of CO-cus will be fairly low due to its weak bonding. Incoming O<sub>2</sub> molecules will dissociatively adsorb on cus-sites (step 1), then react first with CO-cus (step 6) and then either react with CO-bridge (step 7) or transform into more strongly held O-bridge species (step 2) from where reaction according to step 9 takes place. Since under these conditions oxygen adsorption will be rate-limiting,  $r_{\text{CO}_2}$  increases linearly with  $p_{\text{O}_2}$  until a maximum (point A in Figure 2) is reached if the bridge-sites are occupied equally by CO and O. The small CO-bridge residue, seen in curve a of Figure 3, indicates that we only slightly missed the point of equal occupation of the Ru-bridge sites by O-bridge and CO-bridge. This maximum occurs for  $p_{\text{O}_2} = 4 \times 10^{-8}$  mbar (at  $p_{\text{CO}} = 1 \times 10^{-7}$  mbar), suggesting about equal sticking coefficients (probably close to unity) for adsorption of both O<sub>2</sub> and CO.

Upon further increase of  $p_{\text{O}_2}$ , the bridge sites become increasingly occupied by O-bridge so that the formation of CO-bridge and thus reaction step 9 becomes continuously inhibited. The HREEL spectrum recorded at the minimum of  $r_{\text{CO}_2}$  exhibits the presence of both O-bridge and O-cus, but no longer of CO-bridge. CO<sub>2</sub> formation will then only proceed through steps 6 and 8. The concentration of CO-cus will be very low, because of the weak bonding of this species (hence adsorption–desorption according to step 4). As a consequence, after saturation of the O-bridge phase, further increase of  $p_{\text{O}_2}$  will now continuously lead to population of O-cus. The reaction 6 between O-cus and CO-cus is expected to proceed from the beginning (as marked with a dotted line) with lower probability and then eventually also to saturate. Since O-cus was found to occupy at most only about 80% of the cus sites, the latter are not completely blocked for CO adsorption and hence the rate only slowly drops (presumably to zero) even if  $p_{\text{O}_2}$  is increased further. Superposition of the contributions from these parallel reaction steps then accounts for the observed complex kinetic behavior. For our further discussion it is important to note that for  $p_{\text{O}_2} = 1 \times 10^{-7}$  mbar the rate has already decreased to a value typical for reaction 6 (between O-cus and CO-cus) so that we conclude that the reaction has changed from type 9 to type 6 already at this pressure.

Next we discuss the data of Figure 4 which shows the variation of  $r_{\text{CO}_2}$  with  $p_{\text{CO}}$  for fixed  $p_{\text{O}_2} = 1 \times 10^{-7}$  mbar and  $T = 350$  K. At very low  $p_{\text{CO}}$ , the surface is largely covered by both O-bridge and O-cus. Accordingly the HREEL spectrum at point A shows fully developed peaks arising from these two surface species, but no signals from adsorbed CO. Under these conditions essentially only CO-cus and O-cus are expected to be involved in CO<sub>2</sub> formation, i.e., step 6.  $r_{\text{CO}_2}$  will increase proportional to the concentration of CO-cus. Because of its weak binding,  $r_{\text{CO}_2}$  will be low and hence in turn proportional to  $p_{\text{CO}}$ .



This explains the initial linear increase of  $r_{\text{CO}_2}$  with  $p_{\text{CO}}$  (inset of Figure 4). For the temperature dependence of  $r_{\text{CO}_2}$  discussed below, it is important to note the situation for  $p_{\text{CO}} = 1.0 \times 10^{-7}$ : This is just the pressure where the reaction 8 between CO-cus and O-bridge sets in, but the overwhelming part of the reaction takes place still along reaction 6 between O-cus and CO-cus.

With increasing  $p_{\text{CO}}$ , O-cus will be increasingly consumed and also more and more bridge-sites will become oxygen free and thus accessible for the formation of CO-bridge. Since now both channels 6 and 7 for CO oxidation by O-cus are open, the rate increases with  $p_{\text{CO}}$  stronger than before until a maximum is reached where again about equal concentrations of O-bridge and CO-bridge species are expected. Spectrum b in Figure 5 indicates that the system arrived again at the point where there are about equal concentrations of O-bridge and CO-bridge. Following shutting-off the gas supply, the CO oxidation reaction proceeds until all oxygen is consumed and only a small accidental surplus of CO remains.

Further increase of  $p_{\text{CO}}$  then causes increasing concentration of CO-bridge and thereby inhibition of O-bridge formation. Parallel to the suppression of reaction 9 there will however still be parallel occurrence of steps 6 and 7. The weak bonding of CO-cus ascertains that even at higher  $p_{\text{CO}}$  the cus sites will not become completely blocked by CO, and hence the rate decreases only relatively weakly with increasing CO pressure.

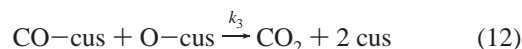
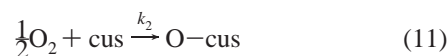
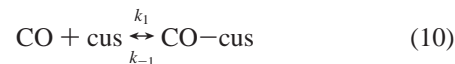
**4.2. Does a “Pressure Gap” Exist?** In a recent study on the oxidation of CO by a catalyst based on RuO<sub>2</sub> particles, prepared from an aqueous solution of RuCl<sub>3</sub> and supported on TiO<sub>2</sub> and SiO<sub>2</sub>, Zang and Kisch<sup>13</sup> reported on remarkable activities down to room temperature. The rate data determined for different temperatures for a gas mixture with  $p_{\text{CO}} = p_{\text{O}_2} = 500$  mbar are included in the Arrhenius plot of Figure 6. Although the authors derived from their four data points (open squares) an activation energy of only about 0.4 eV (= 38 kJ/mol), these data points are fully consistent with the results of the present study obtained for  $p_{\text{CO}} = p_{\text{O}_2} = 10^{-7}$  mbar. It has to be admitted, however, that this agreement so far only holds for the slope ( $\equiv$  activation energy), but not for the absolute scale which should be related to the active surface area. Instead the y-axis in Figure 6 is given in arbitrary units on which both sets of data were arbitrarily displaced vertically until best agreement was reached.

However, we can make an attempt to reach at least an order of magnitude estimate for the absolute reaction rate: The rate data for the single crystal work were quantified according to eq 1 outlined in section 2. Inspection of Figures 2 and 4 reveals that  $r_{\text{CO}_2}$  around the stoichiometric CO:O<sub>2</sub> composition was of the order  $\sim 5 \times 10^{12}$  molecules  $\text{cm}^{-2} \text{s}^{-1}$  at 350 K. Inspection of Figure 6 leads to the conclusion that at room temperature this number will be reduced by about half an order of magnitude so that we arrive at a value of the order  $10^{12}$  molecules  $\text{cm}^{-2} \times \text{s}^{-1}$ .

A rough estimate can, on the other hand, be made for the “real” catalyst. For  $\approx 0.5$  g RuO<sub>2</sub> powder deposited onto SiO<sub>2</sub> with a specific surface area of 340 m<sup>2</sup>/g, an initial rate of CO consumption of 71 mL/min at 300 K was reported.<sup>13</sup> If we assume the same surface area of the catalyst as for the SiO<sub>2</sub> support (i.e., 170 m<sup>2</sup> for 0.5 g) simple arithmetic transforms this number into a rate of CO<sub>2</sub> formation of  $r_{\text{CO}_2} \approx 7 \times 10^{12}$  molecules  $\text{cm}^{-2} \text{s}^{-1}$ . This agreement of the (roughly) estimated activities for both quite different conditions is considered to be rather remarkable.

How can we rationalize that the reaction rate appears to be obviously largely independent of the *total* pressure over 10 orders of magnitude, as long as the same *ratio of partial*

pressures ( $p_{\text{CO}} : p_{\text{O}_2} = 1:1$ ) is established? The measurements on the variation of  $r_{\text{CO}_2}$  with temperature underlying Figure 6 were performed for  $p_{\text{CO}} = p_{\text{O}_2} = 1 \times 10^{-7}$  mbar up to about  $T = 350$  K. Under these conditions the reaction mainly takes place between O-cus and CO-cus with only a minor part occurring between O-bridge and CO-bridge, and the thermal desorption of O-cus is fairly slow. Hence under these conditions the mechanism of the reaction may be approximated as



Justification for the formal description of oxygen adsorption in terms of eqs 11 and 15 has been given above. The rate will be given then by

$$r_{\text{CO}_2} = k_3[\text{CO-cus}][\text{O-cus}] \quad (13)$$

At steady state, we have

$$\frac{d[\text{CO-cus}]}{dt} = k_1 p_{\text{CO}}[\text{cus}] - k_{-1}[\text{CO-cus}] - k_3[\text{CO-cus}][\text{O-cus}] = 0 \quad (14)$$

and within a mean field approximation for the site of O<sub>2</sub> dissociation

$$\frac{d[\text{O-cus}]}{dt} = k_2 p_{\text{O}_2}[\text{cus}] - k_3[\text{CO-cus}][\text{O-cus}] = 0 \quad (15)$$

where [cus], [CO-cus], and [O-cus] are concentration of surface species. We also have

$$[\text{cus}] + [\text{CO-cus}] + [\text{O-cus}] = 1 \quad (16)$$

Because at 350 K the desorption rate of CO is much higher than the production rate of CO<sub>2</sub>, we can omit the term  $k_3[\text{CO-cus}][\text{O-cus}]$  in eq 14. Then eq 14 can be written as

$$\frac{d[\text{CO-cus}]}{dt} = k_1 p_{\text{CO}}[\text{cus}] - k_{-1}[\text{CO-cus}] = 0 \quad (17)$$

Solving eqs 15–17, we get

$$[\text{O-cus}] = \frac{k_2 k_{-1}}{k_3 k_1} \frac{p_{\text{O}_2}}{p_{\text{CO}}} \quad (18)$$

$$[\text{CO-cus}] = \frac{1 - \frac{k_2 k_{-1}}{k_3 k_1} \frac{p_{\text{O}_2}}{p_{\text{CO}}}}{1 + \frac{k_{-1}}{k_1 p_{\text{CO}}}} \quad (19)$$

For  $p_{\text{CO}} = 500$  mbar,  $k_{-1}/k_1 p_{\text{CO}}$  is much smaller than 1, and eq 19 can be simplified to

$$[\text{CO-cus}] = 1 - \frac{k_2 k_{-1} p_{\text{O}_2}}{k_3 k_1 p_{\text{CO}}} \quad (20)$$

For  $p_{\text{CO}} = 10^{-7}$  mbar we estimate the terms  $k_1$  and  $k_{-1} p_{\text{CO}}$  to be of the same order of magnitude, which according to eq 19

decreases the CO concentration and the CO<sub>2</sub> formation rate by less than 1 order of magnitude so that approximation 20 still holds except for the quoted factor. Furthermore, because  $k_1$ ,  $k_{-1}$ ,  $k_2$ , and  $k_3$  are rate constants for elementary steps, it follows in turn that the surface concentrations of O and CO are only given by the pressure ratio of oxygen and CO but not by the absolute pressure of each reactant. Since the overall reaction rate for eq 13 is proportional to [CO-cus] and [O-cus], we can conclude that the reaction rate on this surface will be independent of the total pressure! This conclusion is in full accordance with our suggestion given above that the estimated absolute numbers of CO<sub>2</sub> production in real catalysis and in our UHV steady-state experiment are identical within an order of magnitude although the pressures during reaction differ by more than 10 orders of magnitude. We conclude therefore that a pressure gap does not exist for the CO oxidation at the RuO<sub>2</sub> surface under the discussed conditions (i.e. equal partial pressures and  $T \leq 350$  K). Finally, we add that our model would also work for a different, but quite narrow parameter range, for which the reaction would run on the Ru-bridge sites.

Finally, although we have derived a rather simple expression for the CO<sub>2</sub> formation rate (see eq 13 together with eqs 18 and 20), the activation energy derived from the experimental data of Figure 6 cannot simply be identified with a specific single process, since both  $k_{-1}$  and  $k_3$  enter eq 13 and are expected to be temperature dependent.

## 5. Conclusion

Since the bonding among the surface atoms of a catalyst is usually of comparable strength to that of coupling to the adsorbates involved, a catalytic reaction will in general affect the configuration of these surface atoms, i.e., the reaction “digs its own bed”. The reason for the apparent “pressure gap” in CO oxidation on Ru lies in the fact that there is indeed a “materials gap” involved: Rather high oxygen exposures are required (which will not be attained in regular UHV studies) to establish the catalytically active RuO<sub>2</sub> phase. With the latter the RuO<sub>2</sub> (110) surface grown epitaxially on a Ru(0001) substrate as well as a bulk RuO<sub>2</sub> sample exposing its (110) plane were found to be of comparable reactivity.<sup>12</sup>

In the present study the “pressure gap” could be bridged and remarkable agreement of the kinetic data was found if the

behavior of a RuO<sub>2</sub>(110) single crystal surface, typically operated at 10<sup>-7</sup> mbar pressure, was compared with that of small supported RuO<sub>2</sub> particles working at atmospheric pressure. This could be traced back to the fact that under the conditions discussed the surface is in both cases essentially saturated with about similar fractions of O- and CO-species adsorbed at Ru-cus sites, so that variation of the total pressure (at fixed CO: O<sub>2</sub> ratio) has only little effect. The situation will, however, change if this CO: O<sub>2</sub> ratio is varied, since now participation of the bridge-sites may become more relevant, as well as, at temperatures above ≈350 K, the surface structure may undergo more profound alterations. The results demonstrate again that comparison of catalytic activities is only reasonable in connection with careful analysis of the state of the catalyst's surface; the absolute total pressure may then become irrelevant.

## References and Notes

- (1) (a) Stoltze, P.; Nørskov, J. K. *J. Catal.* **1988**, *110*, 1. (b) Ertl, G. in *Catalytic Ammonia Synthesis*; Jennings, J. R., Ed.; Plenum Press: New York, 1991; p 109.
- (2) (a) Dahl, S.; Senested, J.; Jacobsen, C. J. H.; Törnqvist, E.; Chorkendorff, I. *J. Catal.* **2000**, *192*, 391. (b) Hinrichsen, O.; Rosowski, F.; Muhler, M.; Ertl, G. *Chem. Eng. Sci.* **1996**, *51*, 1683.
- (3) Oh, S. H.; Fischer, G. B.; Carpenter, J. E.; Goodman, D. W. *J. Catal.* **1986**, *100*, 360.
- (4) (a) Lee, H. I.; White, J. M. *J. Catal.* **1980**, *63*, 261. (b) Savchenko, V. I.; Borevskov, G. K.; Kalinka, A. V.; Salanov, A. N. *Kinet. Catal.* **1984**, *24*, 983.
- (5) (a) Cant, N. W.; Hicks, P. C.; Lennon, B. S. *J. Catal.* **1978**, *54*, 372. (b) Kiss, J.; Gonzalez, R. *J. Phys. Chem.* **1984**, *88*, 892.
- (6) Peden, C. H. F.; Goodman, D. W. *J. Phys. Chem.* **1986**, *90*, 1360.
- (7) Over, H.; Kim, Y. D.; Seitsonen, A. P.; Wendt, S.; Lundgren, E.; Schmid, M.; Varga, P.; Morgante, A.; Ertl, G. *Science* **2000**, *287*, 1474.
- (8) Kim, Y. D.; Seitsonen, A. P.; Wendt, S.; Wang, J.; Fan, C.; Jacobi, K.; Over, H.; Ertl, G. *J. Phys. Chem. B* **2001**, *105*, 3752.
- (9) Fan, C. Y.; Wang, J.; Jacobi, K.; Ertl, G. *J. Chem. Phys.* **2001**, *114*, 10058.
- (10) Wang, J.; Fan, C. Y.; Jacobi, K.; Ertl, G. *Surf. Sci.* **2001**, *481*, 113.
- (11) Kim, Y. D.; Seitsonen, A. P.; Over, H. *Phys. Rev. B* **2001**, *63*, 115419; *Surf. Sci.* **2000**, *465*, 1.
- (12) Kim, Y. D.; Over, H.; Krabbes, G.; Ertl, G. *Top. Catal.* **2001**, *14*, 95.
- (13) Zang, L.; Kisch, H. *Angew. Chem.* **2000**, *112*, 4075.
- (14) LaFosse, A.; Wang, Y.; Jacobi, K. Unpublished data.
- (15) Over, H.; Seitsonen, A. P.; Lundgren, E.; Schmid, M.; Varga, P. *J. Am. Chem. Soc.* **2001**, *123*, 11807.